BNL-104765-2014-TECH

AGS/AD/Tech Note No. 349;BNL-104765-2014-IR

IMPEDANCE OF BOOSTER PICKUP ELECTRODES: CALCULATIONS AND COMPARISON WITH MEASUREMENTS

M. Blaskiewicz

April 1991

Collider Accelerator Department

Brookhaven National Laboratory

U.S. Department of Energy

USDOE Office of Science (SC)

DISCLAIMER

Accelerator Division
Alternating Gradient Synchrotron Department
BROOKHAVEN NATIONAL LABORATORY
Upton, New York 11973

Accelerator Division
Technical Note

AGS/AD/Tech. Note No. 349

IMPEDANCE OF BOOSTER PICKUP ELECTRODES: CALCULATIONS AND COMPARISON WITH MEASUREMENTS

M. Blaskiewicz

April 23, 1991

1 ABSTRACT

Numerical estimates of the longitudinal and transverse impedances for the booster capacitive pickup electrode (PUE) are presented. A comparison is made between the calculated longitudinal impedance and the impedance found using a wire measurement.

2 INTRODUCTION

Time domain codes calculate wake potentials while loss factors may be obtained using eigenvalue solvers. For a special, but useful, case the two techniques are simply related [1]. Using a wire measurement, and the supposition

of a lumped impedance, the scattering matrix for a structure may be converted to an impedance. This paper tests the self consistency of the numerical approaches and compares the numerical results with the measurements. The sign and phase conventions are as follows. The wake potentials are defined as

$$\mathbf{W}(\tau) \equiv \lim_{q \to 0} \frac{1}{Qq} \int_{-\infty}^{+\infty} dz \Delta \mathbf{F}(z, \tau + z/v). \tag{1}$$

The source particle has a charge Q while the test particle has a charge q. The particle trajectories are colinear and the test particle lags a distance s behind the source particle. $\Delta \mathbf{F}$ is the total force on the trailing particle minus the force present in a smooth pipe. The impedance is defined as

$$\mathbf{Z}(f) \equiv - \int_{-\infty}^{+\infty} \mathbf{W}(t) e^{-2\pi j f t} dt. \tag{2}$$

3 PUE CALCULATIONS

Time domain calculations for the PUE were done using the MAFIA code T3 [2]. The true geometry and the geometry assumed in the calculations are shown in Figure 1. Since the PUE is symmetric across the $y = 0$ plane, a beam traveling along the z axis will feel no kick in the y direction. Hence, only the portion of the PUE for $y > 0$ was modeled and the beam was taken along the z axis. The time domain code is reliable only for a beam velocity $v = c$; for the booster $v \sim 0.6c$. The stategy for estimating the impedance is as follows.

1) Calculate the wake potentials for $v = c$.

2) Find the eigenmodes which dominate the wake potential.

3) Calculate the impedance at $v = c$ due to these modes.

4) Check for consistency between the two approaches.

5) Use the eigenvectors to estimate the impedance for $v < c$.

The geometry of figure 1a was input to the time domain code T3. The $y = 0$ boundary condition was $E_y = H_x = H_z = 0$, which is the relevant condition for fields which are symmetric with respect to the $y = 0$ plane. Open boundary conditions were used at the boundaries in z. A charge/current source of the form

$$\begin{aligned} \rho &= Q\delta(x)\delta(y)\frac{1}{\sqrt{2\pi\sigma^2}}e^{-\frac{(z-ct)^2}{2\sigma^2}} \\ \mathbf{J} &= \hat{z}c\rho \end{aligned} \tag{3}$$

with $\sigma = 5$ cm was propagated through the cavity and the wake potentials were calculated. The $\hat{x}$ and $\hat{z}$ components of the wake potential are shown in Figure 2. Estimates of the longitudinal and transverse impedance were made by multiplying the wake potentials by a Bartlett window and taking the discrete Fourier transform. The windowing was used to suppress spurious spikes in the impedances, which are shown in Figure 3.

The input geometry of Figure 1a was also used in the eigenvector solver E31 [2]. The $y = 0$ boundary conditions were the same as those used in the time domain, but no open boundary conditions were available for the z direction. Perfectly conducting boundaries were used at the z limits. Five of the eigenmodes had frequencies corresponding to clear spikes in the longitudinal impedance and are given in column 1 of Table 1. The loss parameters k_λ for the five modes were calculated using the Condon method [1] and are shown in column 2 of Table 1, in units of kilovolts per microcoulomb.

The Condon method predicts that the longitudinal wake potential, for a *point* charge moving at $v = c$ through an element with perfectly conducting walls, is given by

$$W_0(s) = H(s) \sum_{\lambda} 2k_\lambda \cos(\omega_\lambda s/c), \tag{4}$$

where ω_λ is the angular frequency for mode λ and $H(s)$ is the Heaviside function. The loss factors are given by

$$k_\lambda = \frac{|V_\lambda|^2}{4U_\lambda} \tag{5}$$

$$V_\lambda = \int E_{\lambda z}(0,0,z) e^{i\omega_\lambda z/c} dz \tag{6}$$

$$U_\lambda = \frac{\epsilon_0}{2} \int |\mathbf{E}(x,y,z)|^2 dx dy dz. \tag{7}$$

To apply equation 4 to our problem the point wake potential must be convolved with the distribution of equation 3 which results in

$$W(s) = \sum_{\lambda} 2k_\lambda F(s, \sigma, \omega_\lambda)$$

$$F(s, \sigma, \omega_\lambda) = \int_0^\infty dy \frac{\cos(\omega_\lambda y/c)}{\sqrt{2\pi\sigma^2}} e^{-\frac{(s-y)^2}{2\sigma^2}} \tag{8}$$

To test whether the modes obtained from E31 were adequate to represent the wake potentials obtained from T3 equation 8 was fitted to the longitudinal wake potential using the frequencies ω_λ from E31 and least squares on the parameters k_λ. The best fit parameters K_λ are shown in column 3 of Table 1. The agreement between the methods is fairly good, considering the fact that the wake potential contains frequencies which are not included in the fit.

Table 1:

f_λ MHz	k_λ	K_λ	$k_\lambda(v = 0.6c)$ kV/μC
273.5	10	9.5	18.5
570.8	4.4	4.6	6.5
1077.3	7.5	8.5	1.8
1496.9	5.5	4.3	.4
1727.6	10	12	1.4

For $v < c$ the output from the time domain solver is unreliable, so the frequency domain was used. In this case the impedance due to coloumb forces also contributes to the longitudinal wake potential. The impedance due to coloumb forces is the result of space charge forces which are present at all regions in the ring and are not well modeled by impulses, so the space charge forces were not included in the PUE impedance estimate.

The loss factors for $v < c$ were calculated using equations 5 through 7 and substituting $0.6c$ for c in equation 6. The loss factors for $v = 0.6c$ are given in column 3 of Table 1.

4 COMPARISON WITH PUE MEASUREMENTS

Transmission line measurements of the longitudinal impedance for the PUE [5] are shown in Figure 4. As is clear from the figure the resonant frequencies and loss factors depend strongly upon the way in which the measurement ports are terminated. For normal operating conditions, the impedance shown in Figure 4b is relevant. One glaring and two less obvious discrepancies between the calculation and the measurement are apparent:

1) the width of the measured resonance is large, while the width of the calculated resonance is essentially zero,

2) the first measured resonant frequency is 230 MHz while the calculated value is 273 MHz,

3) at 273 MHz the calculated loss factor is 10 kV/μC while the measured loss factor is $\sim$ 4 kV/μC.

These discrepancies probably arise because the computer codes require a rather coarse mesh, and do not model resistive material. For instance, the lowest resonant frequency has magnetic field lines which encircle the post that joins the pickup electrode to the outer case. In the actual PUE, the oscillating current in the post encounters a 300 ohm resistive load before reaching the outer case. The broad resonance in the actual PUE is almost certainly due to the external load. Additionally, the coarseness of the numerical mesh required a square post with an effective radius of 7 mm while the wire in the actual pickup has a radius of 1 mm and is sheathed by a dielectric casing of radius 5 mm. The larger inductance in the actual PUE yields a smaller resonant frequency than the numerical model. Order of magnitude calculations for the frequency shift and the Q have been carried out, and bear out these suppositions.

5 CONCLUSIONS

The measured and calculated frequencies of the lowest resonance agree to within $\sim$ 10%, while the loss factors agree within a factor of 2. The measured quality factor is much smaller than the calculated one owing to the presence of external electronics, which cannot be modeled with available computer

codes. The author suggests that the measured impedances be used in beam dynamics calculations. A better estimate might be made by multiplying the measured inpedance by a smooth function that equals $k_\lambda(v = 0.6c)/k_\lambda(v = c)$ at the calculated resonant frequencies.

6 REFERENCES

1. K.L. Bane, P.B. Wilson, & T. Weiland, SLAC-PUB-3528 (1984).

2. R. Klatt, F. Krawczyk, W.R. Novender, C. Palm, T. Weiland, B. Steffen, T. Barts, M.J. Browman, R. Cooper, C.T. Mottershead, G. Rodenz, & S.G. Wipf, SLAC-303 (1986), pp. 276-278.

3. T. Weiland, NIM **212** (1983), pp. 13-34.

4. S.A. Heifets, & S.A. Kheifets, SLAC-PUB-5297 (1990).

5. A. Ratti & T. Shea, private communication.

Figure 1. right (a) Input geometry used in the numerical calculations. The origin of coordinates is in the center of the back plane and the coordinate directions are shown to the left.
left (b) Diagram of actual PUE.

Figure 2. Wake potentials in MKS units for $v = c$. The $\hat{z}$ component is is plotted with overlying squares and the $\hat{x}$ component is the smooth line.

Figure 3. The top figure shows the longitudinal impedance and the $\hat{x}$ component is on the bottom. Both are in units of ohms and the frequency is in Hz. The imaginary part of the impedance is plotted with overlying squares and the real part is smooth.

Figure 4. Transmission line measurements of the longitudinal impedance. The upper panel (a) was obtained using a 50 ohm termination at the end of a $\sim$ 5 cm tuning stub. The lower panel (b) shows the impedance when external electronics used in the booster are in place.

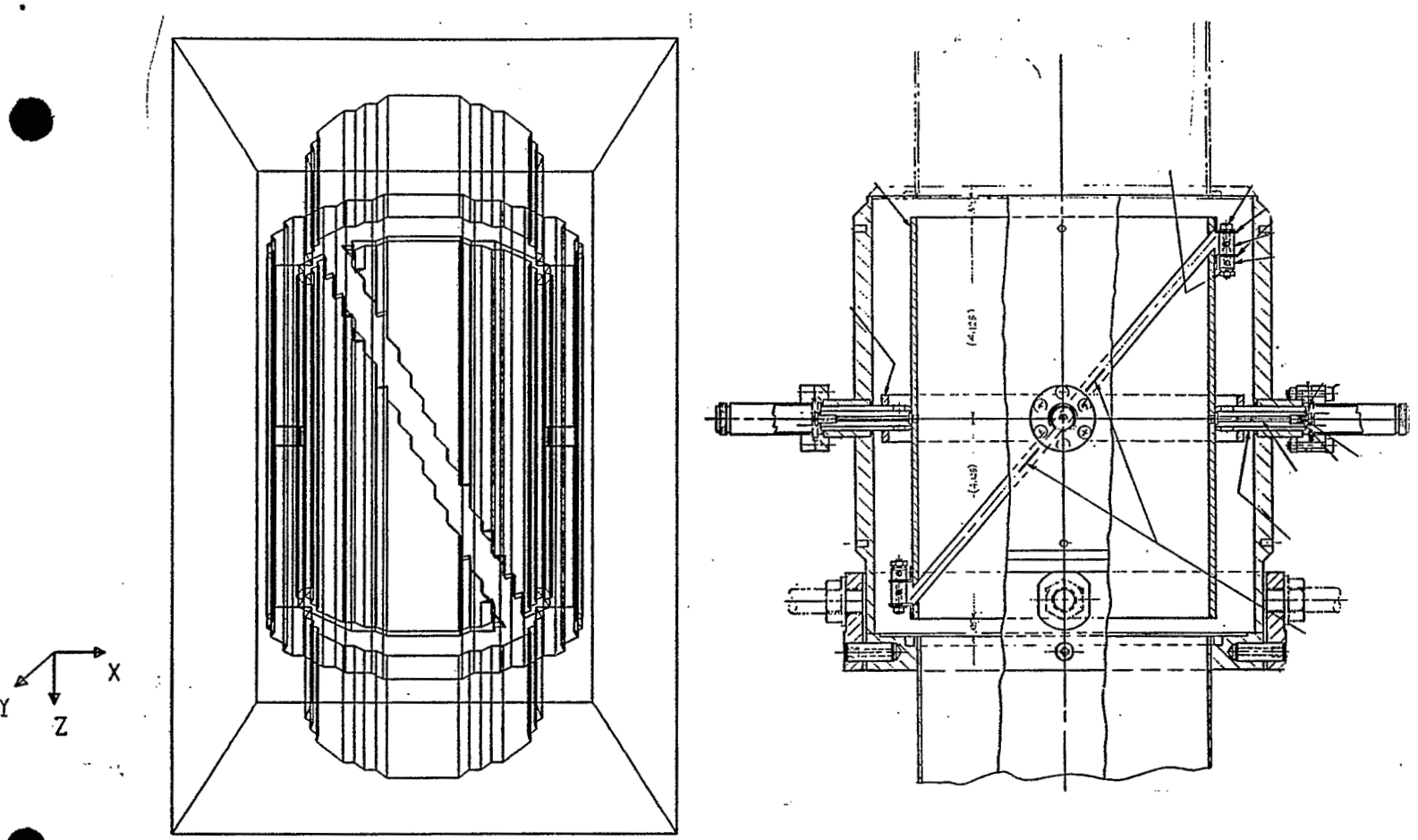

Figure 1. right (a) Input geometry used in the numerical calculations. The origin of coordinates is in the center of the back plane and the coordinate directions are shown to the left.

left (b) Diagram of actual PUE.

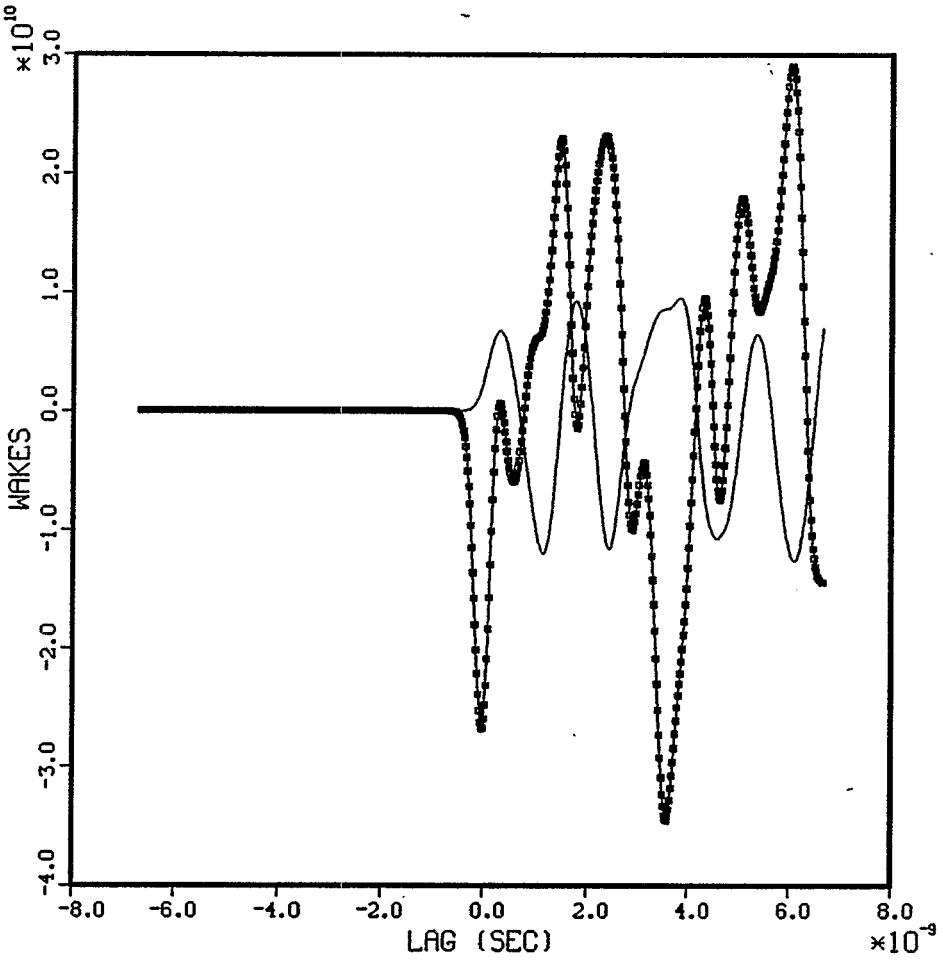

Figure 2. Wake potentials in MKS units for $v = c$. The $\hat{z}$ component is is plotted with overlying squares and the $\hat{x}$ component is the smooth line.

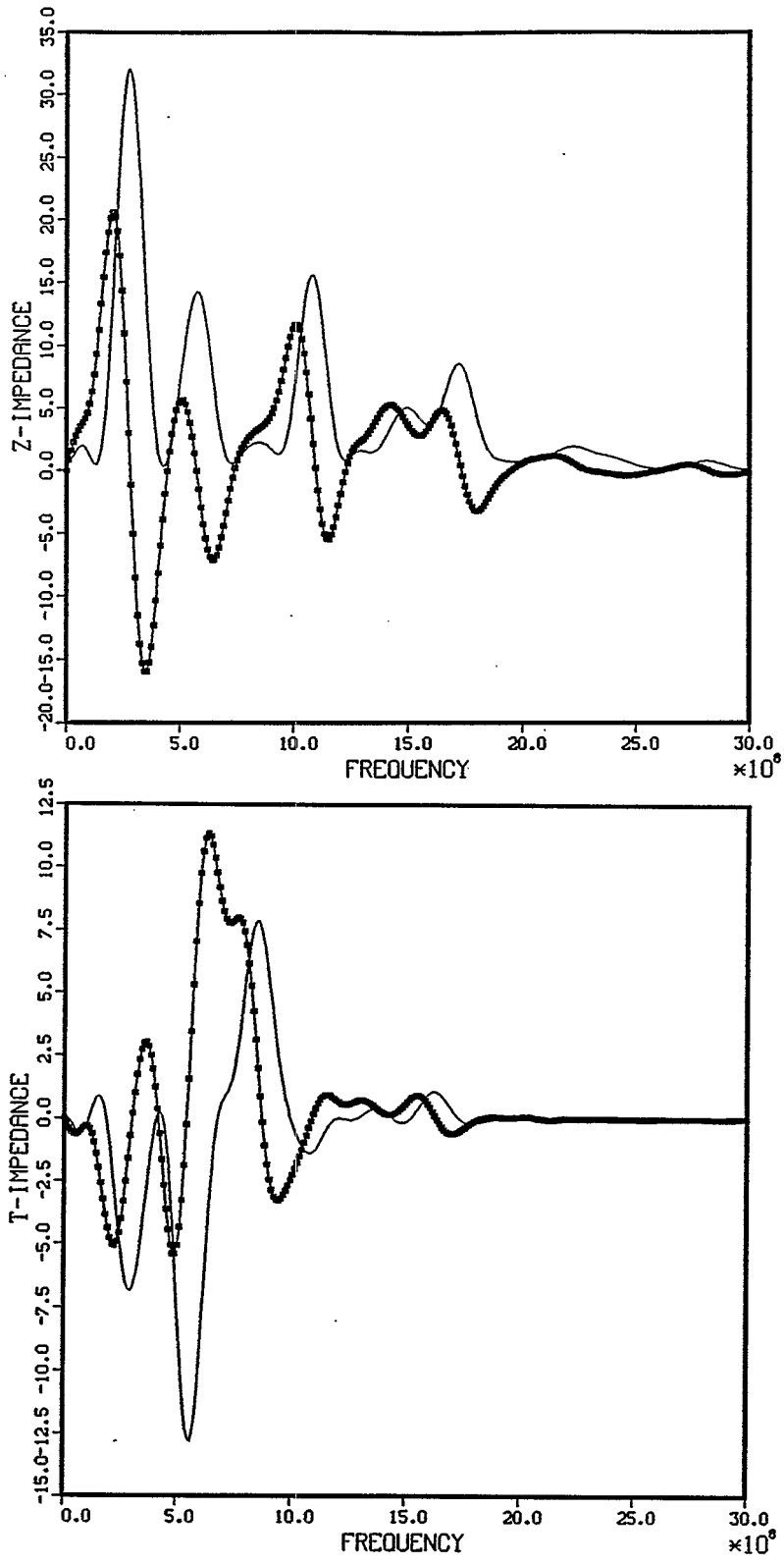

Figure 3. The top figure shows the longitudinal impedance and the $\hat{x}$ component is on the bottom. Both are in units of ohms and the frequency is in Hz. The imaginary part of the impedance is plotted with overlying squares and the real part is smooth.

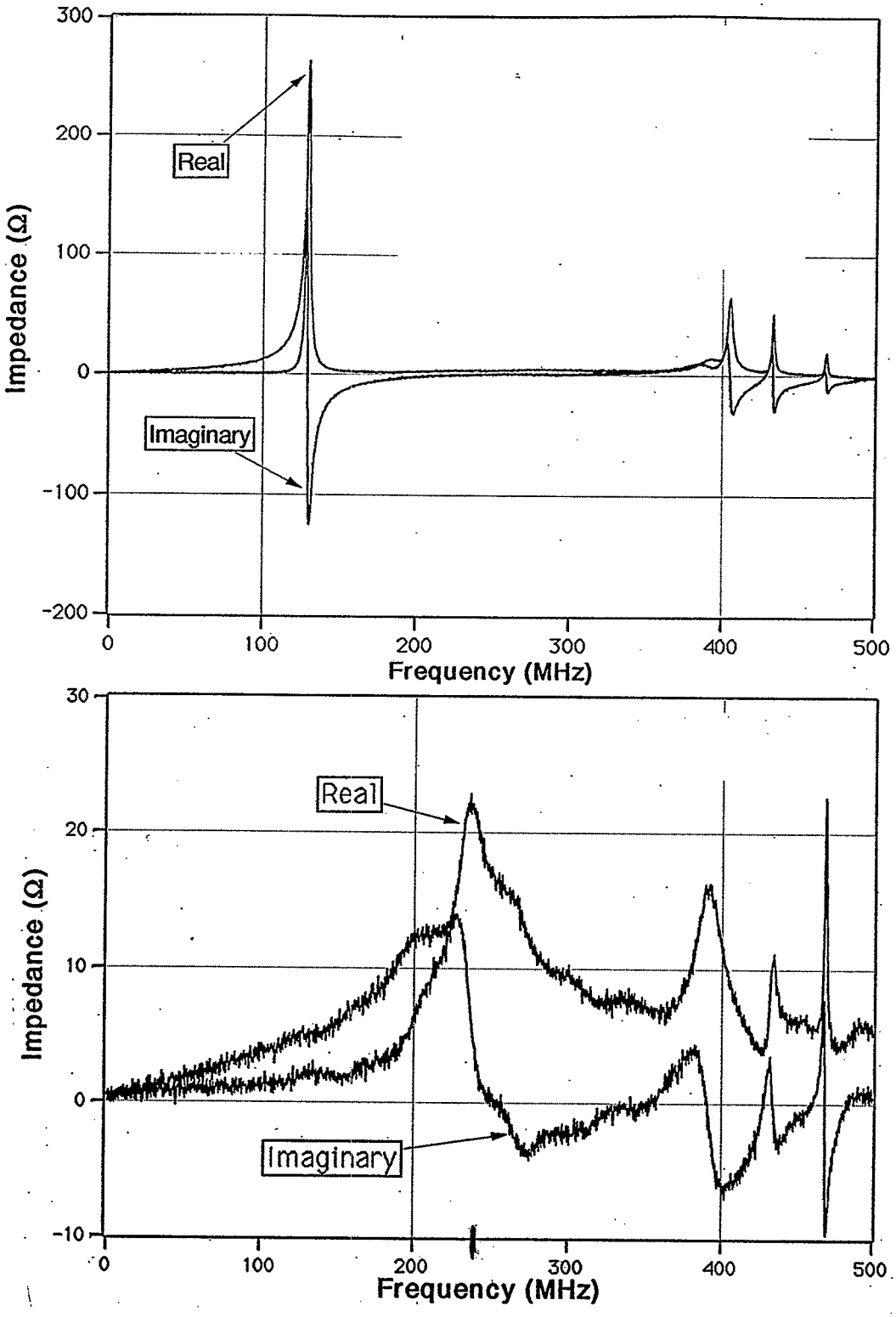

Figure 4. Transmission line measurements of the longitudinal impedance. The upper panel (a) was obtained using a 50 ohm termination at the end of a $\sim$ 5 cm tuning stub. The lower panel (b) shows the impedance when external electronics used in the booster are in place.